

Transient x-ray absorption spectroscopy of hydrated halogen atom

Christopher G. Elles,¹ Ilya A. Shkrob,^{1*} Robert A. Crowell,^{1**}

Dohn A. Arms,² and Eric C. Landahl²

¹ *Chemistry Division, Argonne National Laboratory, 9700 S. Cass Ave, Argonne, IL 60439*

² *Advanced Photon Source, Argonne National Laboratory, 9700 S. Cass Ave, Argonne, IL 60439*

*(Received September *, 2007)*

Time-resolved x-ray absorption spectroscopy monitors the transient species generated by one-photon detachment of an electron from aqueous bromide. Hydrated bromine atoms with a lifetime of ~17 ns were observed, nearly half of which react with excess Br⁻ to form Br₂⁻. The K-edge spectra of the Br atom and Br₂⁻ anion exhibit distinctive resonant transitions that are absent for the Br⁻ precursor. The absorption spectra indicate that the solvent shell around a Br⁰ atom is defined primarily by hydrophobic interactions, in agreement with a Monte Carlo simulation of the solvent structure.

PACS numbers: 78.70.Dm, 78.47.+p, 82.40.-g

Time-resolved x-ray scattering [1] and x-ray absorption (XA) [2-7] measurements provide detailed information about the atomic structure around short-lived species. In this Letter, we report the transient XA spectrum of a simple open shell system, the hydrated Br⁰ atom. Details about the hydration of halogen atoms are not well known, but XA spectroscopy is uniquely suited for probing the interaction of the atom with its aqueous environment. [2,3] The hydration of halogen atoms (X⁰) is very different from the hydration of negatively charged halide anions (X⁻). Whereas the anion forms strong hydrogen bonds with several water molecules in the first solvent shell, [Fig. 1(a)] hydrophobic effects dominate the solvation of neutral halogen atoms. [Fig. 1(b)] There is also evidence that halogen atoms interact directly with a single solvent molecule, leading to an ultraviolet charge transfer (CT) absorption band. [8] The CT absorption promotes an electron from the water molecule onto the halogen atom. In the case of Cl⁰, an electron spin resonance study [9] suggests that the atom forms a two center, three electron ($\sigma^2\sigma^{*1}$) bond with the oxygen atom of a double-donating water molecule [Figs. 1(c)], analogous to the much stronger Cl-Cl bond of Cl₂⁻. [Fig. 1(d)] Similar bonding may also occur for Br⁰ and I⁰ in water. [10]

Recently, Pham *et al.* [7] reported XA measurements of I^0 atoms following biphotonic electron detachment from aqueous iodide. They observe a prominent change of the XA spectrum at the L_1 and L_3 absorption edges, but their interpretation is complicated by the reaction of I^0 with excess I^- to form a substantial amount of I_2^- and I_3^- within the ~ 80 ps duration of the x-ray pulse. Rapid formation of molecular anions in their experiment is a consequence of the high concentration of I^- (500 mmol/dm^3) that is necessary to overcome inefficient two-photon absorption. In contrast, efficient one-photon electron detachment from Br^- at 200 nm [11] and strong XA at the K-edge of bromine allow us to use dilute aqueous solutions in which the reaction of Br^0 with excess anions is much slower.

The present experiment uses the laser pump – x-ray probe capabilities of beamline 7ID of the Advanced Photon Source. Fourth harmonic generation of the output from an amplified Ti:sapphire laser provides 5 μJ pulses of 200 nm light with a repetition rate of 1 kHz. A MgF_2 lens focuses the ultraviolet light to a diameter of 95 μm at the sample, where it crosses the x-ray beam at an angle of 4° . The laser is synchronized with the synchrotron by an active feedback control loop that adjusts the laser oscillator cavity length and the relative delay between laser and x-ray pulses is controlled electronically. The synchrotron provides tunable x-ray pulses with a duration of ~ 80 ps and a repetition rate of 6.54 MHz (24 bunch mode). X-rays from the undulator pass through a tunable diamond monochromator ($\Delta E/E = 5 \times 10^{-5}$) before a Kirkpatrick-Baez mirror pair focuses them to a spot size of about 25 μm in the sample. The sample is a 100 μm thick liquid jet of 5-10 mmol/dm^3 NaBr solution with the flat surface of the jet rotated 45° relative to the x-ray beam. Se filters absorb elastically scattered x-rays and a gated avalanche photodiode detector on each side of the jet monitors the bromine K_α fluorescence. We record fluorescence count rates for the two x-ray pulses immediately following the laser pulse (Δt , $\Delta t + 153$ ns) and normalize the signal to account for variations of the x-ray flux. Scanning the incident energy gives the XA spectrum at each delay time.

Fig. 2(a) compares the static XA spectrum of the bromide solution with the transient spectrum at 1 ns delay. The conversion of a fraction of Br^- anions to neutral Br^0 atoms by the 200 nm laser pulse is evident from the resonant $1s-4p$ transition below the bromine K-edge. Subtracting the static spectrum of Br^- from the transient spectra at

delays of 1 and 154 ns gives the difference spectra $\mu_{on} - \mu_{off}$ in Fig. 2(b). The spectrum is different at the two delay times because nearly half of the Br^0 atoms at 1 ns react with excess Br^- to form Br_2^- by 154 ns, while most of the other Br^0 atoms recombine with the hydrated electron. Other than Br^- , the predominant species at 1 ns and 154 ns are Br^0 and Br_2^- , respectively. [12] The resonant transition in Br_2^- is 1.6 eV higher in energy than the transition in Br^0 , [Fig. 2] where the difference is largely due to splitting of the bonding (σ_g) and antibonding (σ_u^*) molecular orbitals relative to the atomic $4p$ orbital. [Fig 1(d)] Excitation of Br^0 promotes a $1s$ electron into the $4p$ vacancy produced by detaching an electron from Br^- , whereas the resonant transition for the Br_2^- anion excites an electron to the σ_u^* antibonding orbital. The optical transition energies for π_g - σ_u^* and σ_g - σ_u^* excitation are 1.7 and 3.4 eV, respectively, [13] confirming that the 1.6 eV shift of the XA band comes predominantly from the splitting of the molecular orbitals rather than a shift of the relative $1s$ orbital energy from Br^0 to Br_2^- .

The 1.6 eV spectral shift of the resonant XA band allows us to observe the reaction kinetics. Fig. 3 shows the time-dependent change in absorption at 13.473 and 13.476 keV. Predominantly Br^0 atoms absorb at the lower energy, therefore the decay of the absorbance indicates the loss of Br^0 atoms as they recombine with hydrated electrons and react with Br^- . Although Br^0 also contributes to the 13.476 keV absorption at short delay times, that signal increases on the timescale of the Br^0 decay due to production of Br_2^- . Details of the kinetic scheme and calculations of the conversion yields are given as supplemental material. [12] The kinetics give accurate estimates of the product concentrations and thus allow us to reconstruct the spectra of the transient species by subtracting the contribution from Br^- . These spectra are shown in Fig. 2(c), along with the spectrum of Br^- . The K edge absorption energy is ~ 5 eV higher for the transient species than for bromide. The higher energy for Br^0 reflects the electrostatic attraction of the outgoing electron to the positively charged core. A similar shift of ~ 5 eV for the absorption edge of Br_2^- is somewhat surprising given the negative charge of the diatomic anion and likely reflects solvent screening and delocalization of the valence electron.

The large reduction in the modulation depth for the Br^0 atom relative to the Br^- anion is perhaps the most intriguing feature of the recovered XA spectrum. A Monte Carlo (MC) simulation of the solvent structure provides helpful insight to understand the

difference in the XA fine structure (XAFS) above the K edge. The simulation includes 200 SPC/Flex water molecules [14] and a single Br^0 or Br^- in a supercell, with solute-water interaction potentials from refs. [15] and [10], respectively. An ensemble of 1500 snapshots at 298 K were taken from 3×10^7 MC steps to give the Br-O radial distribution functions (RDF), $g_{\text{Br-O}}(r)$, in Fig. 4(a). (The proton contribution to the XAFS spectrum is negligible.) For Br^- , the narrow peak at 3.2 Å is due to strong hydrogen bonding ($\text{Br}^- \cdots \text{H-OH}$) between the anion and ~ 6 water molecules in the first solvent shell. [15,16] The RDF for the Br^0 atom lacks this feature because the hydrophobic atom interacts weakly with the solvent. Instead, the atom occupies a nearly spherical cavity formed by 10-12 water molecules that are hydrogen bonded to other water molecules in the first and second solvent shells. The only distinctive feature in this RDF is a shoulder at 3 Å that corresponds to a weak $\text{Br}^0 \cdots \text{OH}_2$ adduct involving a single water molecule. For other water molecules, the Br^0 -O distances are significantly longer, ~ 3.7 Å.

For further insight, we simulate the XAFS spectra of Br^- and Br^0 [Fig. 4(b)] using the program FEFF8 [17] and nuclear configurations of water molecules with $r(\text{Br-O}) < 8$ Å from the MC ensemble. The highly organized hydrogen bonding structure of hydrated Br^- gives deep oscillations in the static spectrum, but the magnitude of the oscillations is ~ 10 times smaller for hydrated Br^0 atoms. Although the calculation pertains to higher XA energies than the present experiment covers, the modulation is clearly much weaker in the reconstructed spectrum of Br^0 than in the Br^- spectrum. [Fig. 2(c)] The contribution from the $\text{Br}^0 \cdots \text{OH}_2$ complex is small compared with the contributions from the other 10-12 O atoms in the first solvent shell and therefore does not give a strong XAFS signal.

Pham *et al.* [7] suggest that significant CT from a water molecule suppresses the $2s$ - $5p$ resonance in the L_1 spectrum of I^0 by as much as 70%. No such suppression of the $1s$ - $4p$ resonance is evident from our K-edge spectrum of Br^0 . To estimate the degree of CT in the Br^0 -water adduct, water clusters with $r(\text{Br}^0\text{-O}) < 5.5$ Å were extracted from the MC simulation. Water molecules outside of the extracted cluster were replaced by fractional point charges and Hartee-Fock calculations of the "embedded" clusters using a 6-311++G** basis set give a Mulliken charge of $-(0.07-0.08)$ on the Br^0 atom, which would suppress the pre-edge feature very little.

In conclusion, we report the transient XA spectrum of the short-lived hydrated Br^0 atom and monitor its reaction to form Br_2^- . The solvent shell around Br^0 is defined primarily by weak hydrophobic interactions, with the atom residing at the center of a large “bubble.” A single solvent molecule directly interacts with the atom to form a $\sigma^2\sigma^{*1}$ bond, but its XAS signature is obscured by 10-12 unbound water molecules. Calculations indicate that CT in the ground state of the Br-water adduct is too weak to suppress the $1s-4p$ resonance. We thank S. Ross for help with APD detectors, E. Dufresne and D. Walko for beamline assistance, L. Young and her colleagues for use of their instruments, and P. Jungwirth, C. Bressler, R. Saykally, and P. D’Angelo for helpful discussions. Use of the Advanced Photon Source was supported by the U.S. Department of Energy, Office of Basic Energy Sciences, under Contract No. DE-AC02-06CH11357.

* shkrob@anl.gov, ** rob_crowell@anl.gov

- [1] A. Plech *et al.*, Phys. Rev. Lett. 92, 125505 (2004)
- [2] C. Bressler *et al.*, J. Chem. Phys. 116, 2955 (2002)
- [3] C. Bressler and M. Chergui, Chem. Rev. 104, 1781 (2004)
- [4] L. X. Chen, Angew. Chem. Intl. Ed. 43, 2886 (2004)
- [5] W. Gawelda *et al.*, Phys. Rev. Lett. 98, 057401 (2007)
- [6] T. Lee *et al.*, J. Chem. Phys. 122, 1 (2005)
- [7] V.-T. Pham *et al.*, J. Am. Chem. Soc. 129, 1530 (2007)
- [8] A. Treinin and E. Hayon, J. Amer. Chem. Soc. 97, 1716 (1975).
- [9] M. D. Sevilla *et al.*, J. Phys. Chem. A 101, 2910 (1997)
- [10] M. Roeselova, U. Kandor, and P. Jungwirth, J. Phys. Chem. A 104, 6523 (2000)
- [11] R. Lian *et al.*, J. Phys. Chem. A 110, 9071 (2006).
- [12] See EPAPS Document No. ***** for supplementary information. This document can be reached via a direct link in the online article's HTML reference section or via the EPAPS homepage (<http://www.aip.org/pubservs/epaps.html>).
- [13] D. Zehavi and J. Rabani, J. Phys.Chem. 76, 312 (1972).
- [14] Y. Wu, H. L. Tepper, and G. A. Voth, J. Chem. Phys. 124, 024503 (2006).

- [15] P. D'Angelo *et al.*, J. Chem. Phys. 100, 985 (1994)
[16] P. J. Merklings *et al.*, J. Chem. Phys. 119, 6647 (2003).
[17] A.L. Ankudinov *et al.*, Phys. Rev. B 58, 7565 (1998).

Figure captions.

FIG 1. Sketches of the solvation structure around (a) Br^- and (b) Br^0 . Panels (c) and (d) show the schematic orbital diagrams for $\text{Br}^0 \cdots \text{OH}_2$ complex and Br_2^- , respectively

FIG 2 (color online). (a) Laser-on and laser-off x-ray absorption spectra from aqueous Br^- , for $\Delta t = 1$ ns. The inset shows the static spectrum of Br^- . (b) The difference spectra $\mu_{on} - \mu_{off}$ at delay times of 1 ns (open circles) and 154 ns (filled squares). (c) Reconstructed XA spectra of Br^0 (open circles) and Br_2^- (filled squares). The solid line is the absorption spectrum of Br^- . Vertical bars indicate 95% confidence limits.

FIG 3. Transient XA difference $\mu_{on} - \mu_{off}$ signals for 9.8 mmol/dm³ solution of NaBr observed at 13.473 keV (open circles) and 13.476 keV (filled squares). The lines are to guide the eye.

FIG 4 (color online). (a) Calculated Br-O RDF for hydrated Br^- and Br^0 . Oxygen coordination numbers N are indicated by arrows. The inset shows the singly occupied orbital of the bromine atom inside the "embedded" water cluster from our *ab initio* calculations. (b) The simulated XAFS spectra for hydrated Br^- and Br^0 . The first oscillation corresponds to the energy range of Fig. 2(c).

Figure 1, Elles et al.

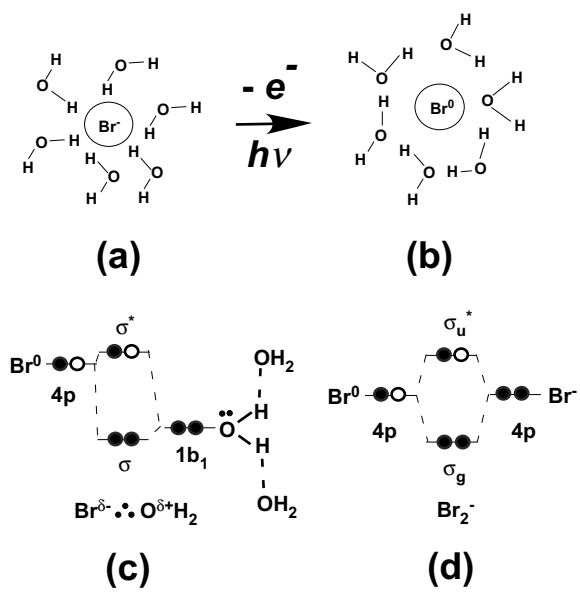


FIG 2, Elles et al.

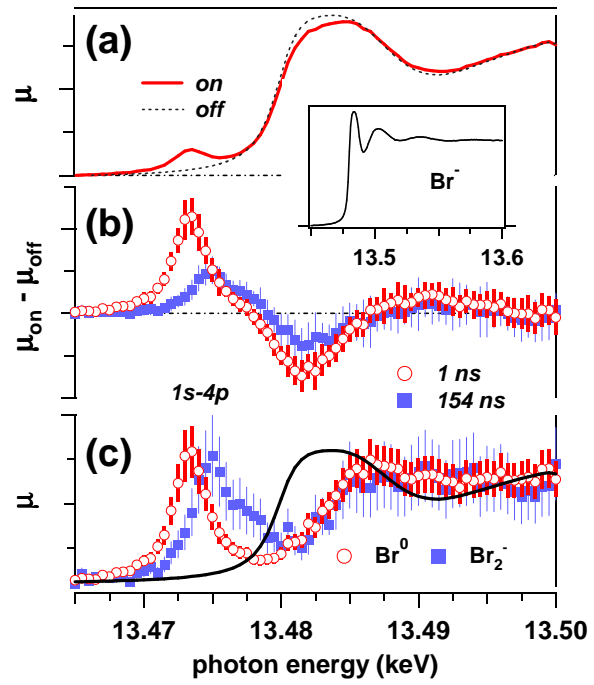


FIG 3, Elles et al.

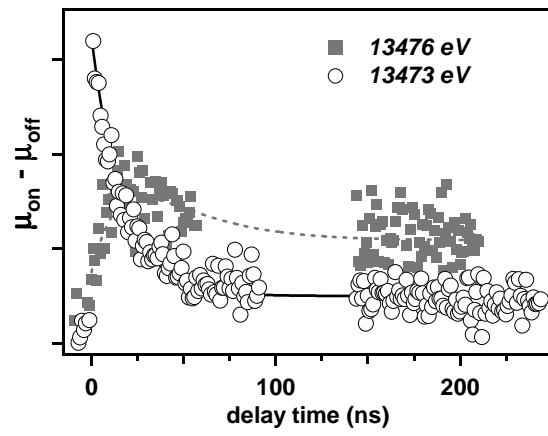
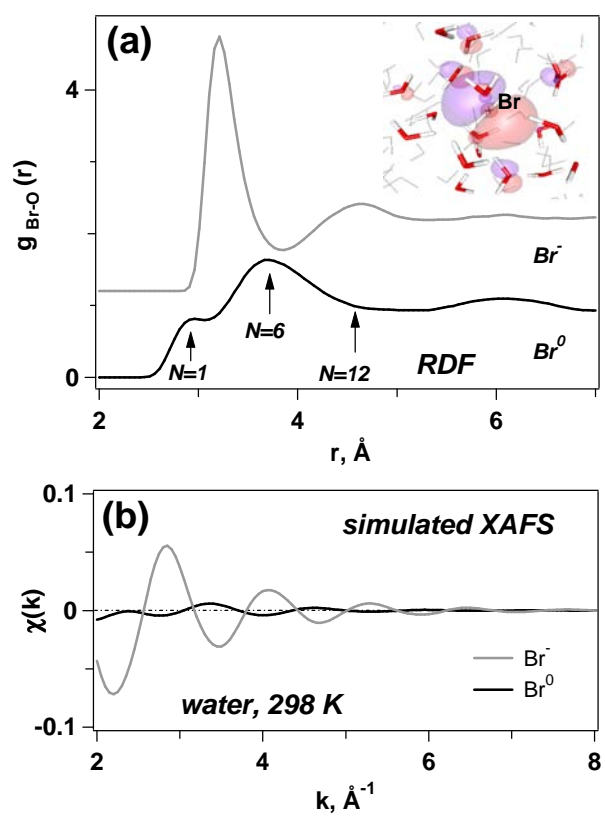


FIG 4, Elles et al.



Supplemental Information

Transient x-ray absorption spectroscopy of hydrated halogen atom

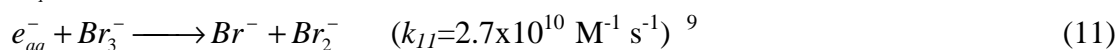
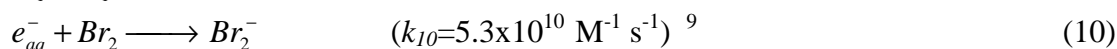
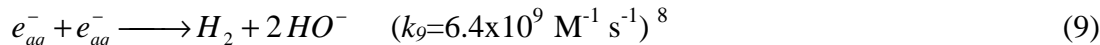
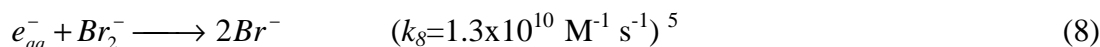
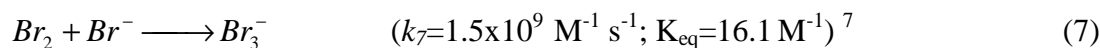
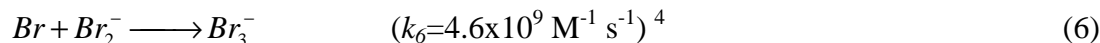
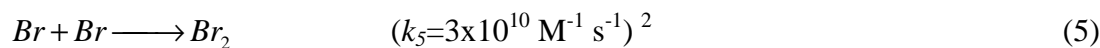
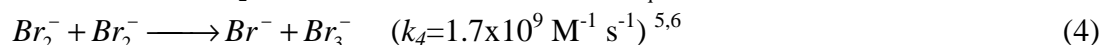
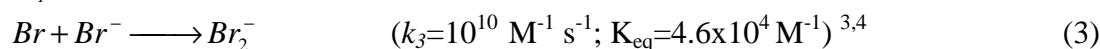
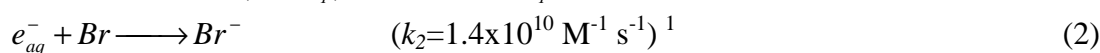
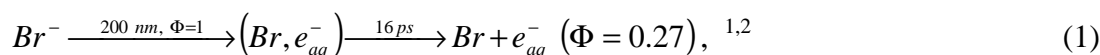
C. G. Elles,¹ I. A. Shkrob,¹ R. A. Crowell,¹ D. A. Arms,² E. C. Landahl,²

¹ Chemistry Division, Argonne National Laboratory, 9700 S. Cass Ave, Argonne, IL 60439;

² Advanced Photon Source, Argonne National Laboratory, 9700 S. Cass Ave, Argonne, IL 60439

e-mail: shkrob@anl.gov, rob_crowell@anl.gov

Reaction scheme 1. (1 M = 1 mol/dm³ = 6x10²⁰ cm⁻³)



This reaction scheme was used to calculate time dependent concentrations of the transient species shown in Figure 1S and other analyses. The only variable input parameter is the initial photoconversion of the Br⁻ to free Br⁰ atoms. For iodide, reaction (7) has equilibrium constant of 750 M⁻¹, and the formation of I₃⁻ is a major complication. For bromide, the yield of Br₃⁻ is insignificant, as the equilibrium is shifted towards Br₂ at the low concentration of the bromide (< 10 mM). The yield of Br₂ is much lower than the yield of the Br₂⁻ due to the occurrence of rapid reaction (10).

For 4.9 mM Br⁻ solution (conditions for the data shown in Figure 2), the estimated ratio [Br₂]/[Br₂⁻]≈0.13 at the delay time of 154 ns (that approximately corresponds to the maximum yield of the Br₂⁻) and [Br⁰]≈0, so the spectrum is dominated by the Br₂⁻. At the delay time of 1 ns, [Br₂]/[Br⁰]≈0.06 and [Br₂⁻]/[Br⁰]≈0.09, and the spectrum is mainly from the Br⁰.

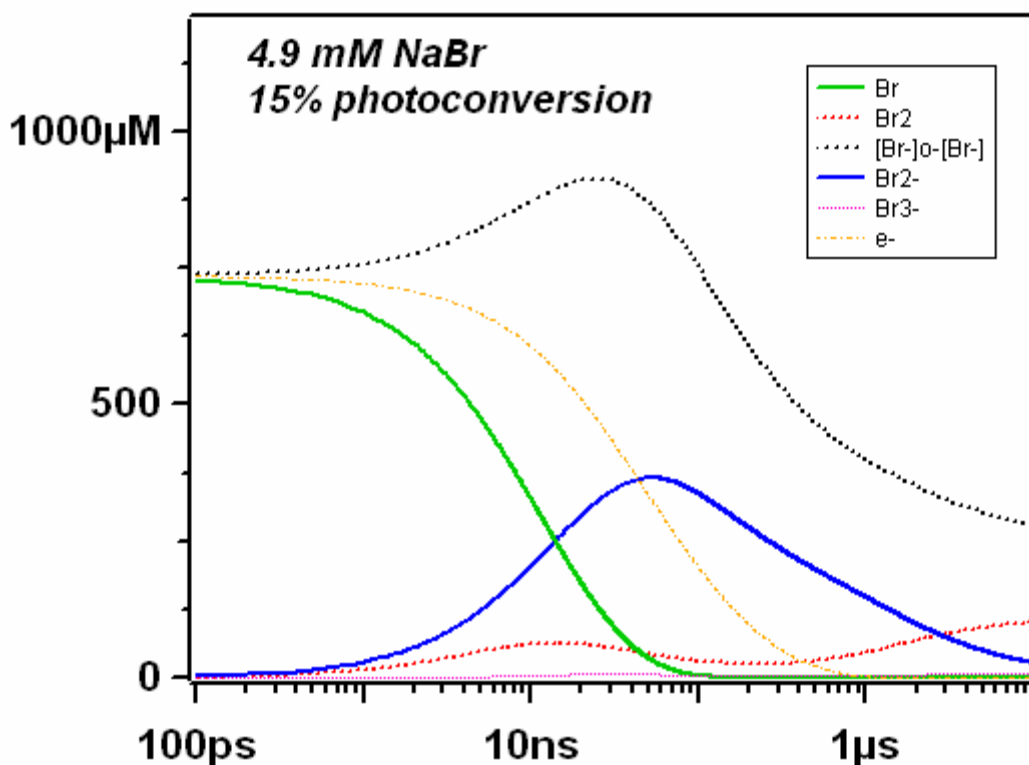


FIG 1S. Simulated kinetics of bromine containing species in an aqueous solution, for 15% initial photoconversion of 4.9 mM Br^- to free Br^0 atoms.

The decay kinetics of the Br^0 are mainly via reactions (2) and (3). Due to the occurrence of bimolecular reaction (2) in the bulk, the apparent rate constant $k_{-\text{Br}}$ of the Br^0 atom decay increases as $[\text{Br}^0]$ increases. For 9.8 mM Br^- solution, we obtained $(6.2 \pm 0.4) \times 10^7 \text{ M}^{-1} \text{ s}^{-1}$ (Figure 3) which is significantly greater than $k_3[\text{Br}^-]$. Using the calculated $k_{-\text{Br}}$ vs. photoconversion efficiency as a calibration plot allowed us to estimate the photoconversion as 12-15%. For this photoconversion, the calculated ratio of $[\text{Br}_2^-]$ at 154 ns and $[\text{Br}^0]$ at 1 ns is 0.45-0.48, which is close to the experimental ratio of the *Is-4p* peak amplitudes (0.43-0.47). Direct calculation of the photoconversion using the extrapolated quantum yield at 1 ns (≈ 0.29)¹ and the extinction coefficient of the Br^- at 200 nm ($10^4 \text{ M}^{-1} \text{ cm}^{-1}$) that included depletion of the laser light along the optical path and laser beam refraction in the sample ($n=1.4$) gave the estimate of 13% at $[\text{Br}^-]=9.8 \text{ mM}$ for the 200 nm laser power of 4.7 μJ .

References for the reaction scheme:

1. The rate constant k_2 in the water bulk was estimated from picosecond geminate recombination kinetics obtained for the hydrated electron (e_{aq}^-) in Ref. 11 of the paper. The rate constant of reaction (2) is given by $k_2 = 4\pi n R_{\text{eff}} D$, where D is the

mutual diffusion constant and $R_{eff} = a(1 - p_d)$ is the effective radius of recombination, which is the product of the Onsager radius a for the potential well (that exists due to the weak attraction between hydrated Br^0 and e_{aq}^-) and $(1 - p_d)$, which is the probability of recombination. The Onsager radius can be estimated from the dimensionless parameter $\alpha = ap_d \sqrt{W/D}$ that was estimated to be 0.57 in Ref. 11 by fitting the geminate recombination kinetics observed for the hydrated electron; the rate constant W in the expression for this parameter is the reciprocal residence time of the geminate pair inside the potential well (that was estimated to be ca. 16.5 ps in Ref. 11). For the reported $D=4.5 \times 10^{-5} \text{ cm}^2/\text{s}$, $a=5.8 \text{ \AA}$, and $p_d=0.27$, we obtain $R_{eff}=4.2 \text{ \AA}$ and $k=1.4 \times 10^4 \text{ M}^{-1}\text{s}^{-1}$. The terminal quantum yield Φ of the e_{aq}^- (attained by the completion of the geminate recombination stage) for 193 nm photoexcitation of aqueous Br^- is 0.365 (as determined by nanosecond laser photolysis by M. C. Sauer *et al.* J. Phys. Chem. A 108, 5490 (2004)). The estimate of $\Phi \approx 0.27$ for 200 nm photoexcitation of the bromide was obtained in picosecond laser photolysis experiment in Ref. 11.

2. The rate constant for recombination of two aqueous I^0 atoms was taken from A. J. Elliot, Can. J. Chem. 70, 1658 (1992)
3. D. Zehavi and J. Rabani, J. Phys. Chem. 76, 312 (1972)
Y. Liu *et al.*, J. Phys. Chem. A, 106, 11075 (2002).
4. J. Lind *et al.*, J. Am. Chem. Soc. 113, 4629 (1991)
5. M. S. Matheson *et al.*, J. Phys. Chem., 70, 2092 (1966)
6. B. G. Ershov *et al.*, Phys. Chem. Chem. Phys., 4, 1872 (2002)
7. M.-F. Ruasse *et al.*, J. Phys. Chem. 90, 4382 (1986).
8. K. H. Schmidt and D. M. Bartels, Chem. Phys. 190, 145 (1995).
9. H. A. Schwarz and P. S. Gill, J. Phys. Chem. 81, 22 (1977).